JOURNAL OF APPLIED ELECTROCHEMISTRY 14 (1984) 9–14

Dielectric characteristics of miniature aluminium electrolytic capacitors under stressed voltage conditions

J. M. ALBELLA, C. GÓMEZ-ALEIXANDRE, J. M. MARTINEZ-DUART

Instituto Física Estado Sólido (CSIC) and Dpt. Física Aplicada, C-XII, Universidad Autónoma, Cantoblanco, Madrid 34, Spain

Received 11 January 1983

The effects of applying voltages higher than the nominal voltage V_N, for given periods of time, to miniature aluminium electrolytic capacitors has been investigated. The measurements of the current transients, the I–V characteristics, and the a.c. properties indicate that the main effect of subjecting the capacitors to the high voltages is an irreversible change in the capacitor dielectric characteristics as a consequence of a large increase in the resistance of the electrolyte and in the permanent leakage current through the anodic oxide. This current, very noticeable for voltages higher than V_N, is attributed to an electronic conduction mechanism in an avalanche regime. The measured dielectric parameters and their evolution after exposing the capacitors to stressed voltage conditions are interpreted in terms of an extension of McLean's equivalent circuit for an electrolytic capacitor.

1. Introduction

The I–V characteristics of aluminium electrolytic capacitors show in most cases two well differentiated regions. For low voltages, i.e. for V smaller than the nominal voltage V_N, the conduction through the anodic oxide generally obeys a Schottky or Poole–Frenkel mechanism [1, 2]. On the other hand, for $V > V_N$, it has been shown that $I \propto \exp(V)$, suggesting that for this voltage range the current is due to the transport of ions under the action of the applied electric field [3].

Although the rate of failure of aluminium electrolytic capacitors at high voltages can be investigated by a careful observation of the I–V characteristics [4], there is a lack of published results in this voltage region. In this paper, we study the I–V characteristics, especially at high voltages, and the effect on the dielectric properties of applying to the capacitors voltages higher than V_N during specified time intervals. The resulting changes in the capacitor properties are interpreted in terms of the damage caused to the dielectric by the applied high fields and the degradation of the electrolyte as a consequence of the transport of electronic charge, in an avalanche regime, through the capacitor.

2. Experimental details

Standard aluminium electrolytic capacitors of the miniature type, with capacitances in the range of 33 to 100 μF and nominal voltages up to 40 V were used in this work. The electrolyte of the capacitors, having a resistivity of 80 ohm cm, consisted of a mixture of boric acid, picric acid and benzoquinone dissolved in ethylene glycol. In addition, ammonia was added to the electrolyte until the pH reached a value of about 5.5. The $I = I(t)$ transients, at a given voltage, were recorded during a time interval of one hour by means of a Keithley model 155 electrometer. The recording of transients was started at 5 V and followed by the recording of transients at 10, 15, 20 V, etc., to a voltage of about 1.5 V_N. Therefore, in each case, the polarization (voltage x time) to which each capacitor had been exposed is well specified. After subjecting the capacitors to a given polarization, the dielectric properties were measured with a Hewlett Packard model 4274A LCR meter in the 0.1–100 kHz frequency range.

0021-891X/84 $03.00 + .12.

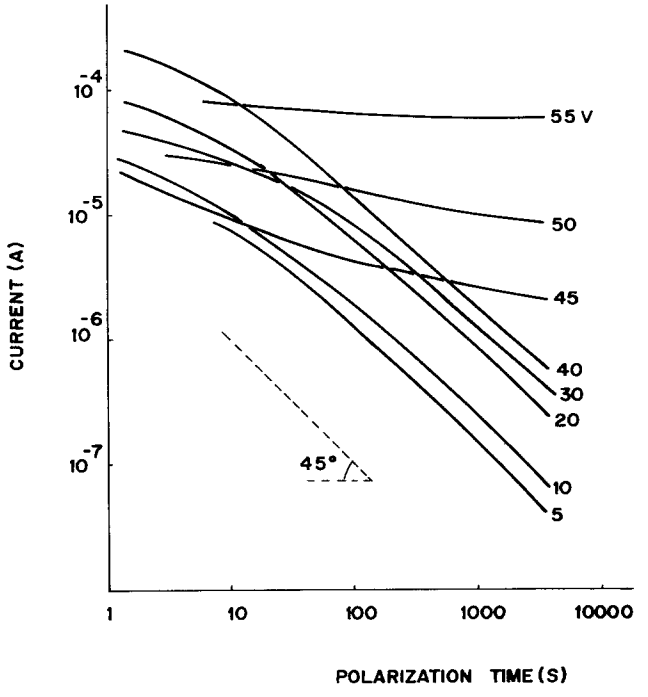

Fig. 1. Current transients for a miniature 100 μF/40 V capacitor.

3. Results

3.1. $I = I(t)$ transients and I–V characteristics

Fig. 1 shows the typical transients $I = I(t)$ on a log–log scale for a 100 μF/40 V miniature aluminium electrolytic capacitor. Two types of curves can be clearly distinguished in Fig. 1 depending on the value of the polarization voltage. In the low voltage region ($V \lesssim V_N$), and a few seconds after applying the polarization voltage, the dependence $I = I(t)$ is close to a relation of the type

$$I(t) \propto t^{-n} \qquad (1)$$

with $n \lesssim 1$. It is also observed that, for the time interval considered in Fig. 1, the value of the current does not reach a stationary value. On the other hand, in the high voltage region ($V \gtrsim V_N$), the current transients show a different behaviour. In effect, it can be observed in Fig. 1 that, as V approaches and exceeds V_N, the slope of the $I = I(t)$ curves in the log–log scale starts to approach zero. In fact, for $V > 55$ volts, the current slowly increases with time (not shown in Fig. 1). The high voltage region is therefore characterized, after a few minutes of applying the voltage, by a slowly decreasing value of the current which, as expected, is much larger than the values at low voltages. However, for short polarization times, the value of the current is smaller than the respective values in the low voltage region. Since the transients, at a given voltage, were recorded after subjecting the capacitor for one hour to the preceding value of V in Fig. 1, the low values of the

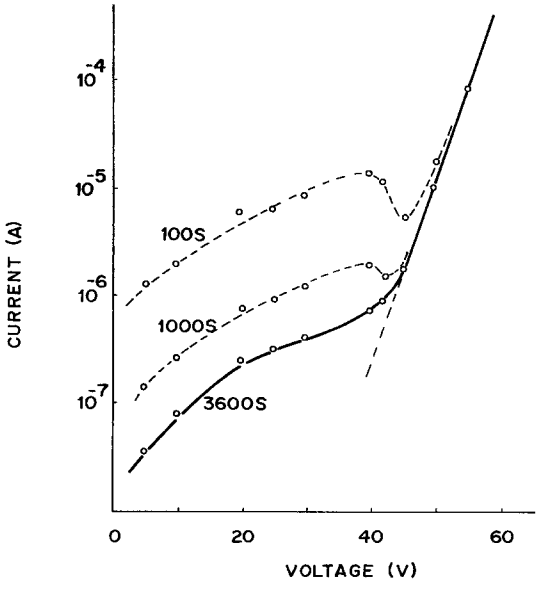

Fig. 2. I–V characteristics for the capacitor of Fig. 1 taken at 100, 1000 and 3600 s.

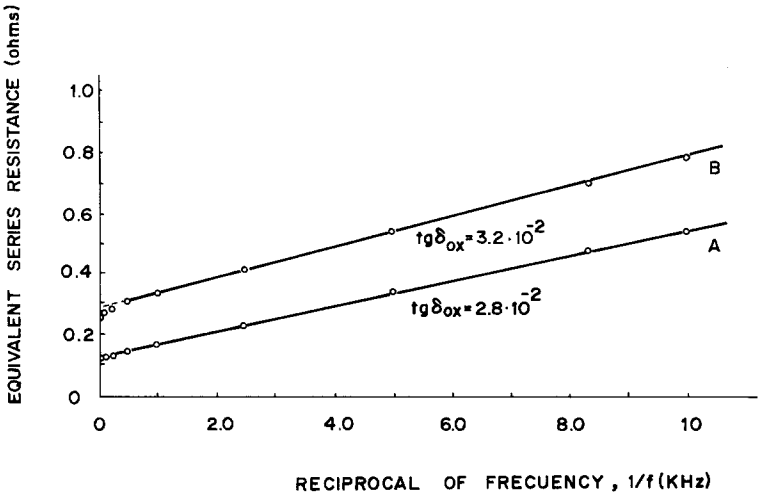

Fig. 3. ESR against reciprocal of frequency before (curve A) and after (curve B) recording the transients of Fig. 1.

initial current through the capacitors on the high voltage region can be attributed to an increase in the equivalent series resistance with the polarization time.

In addition to the transients, the analysis of the I–V characteristics is very useful in the interpretation of the conduction mechanisms across the oxide in the capacitor. Fig. 2 shows a plot of $\log I$ against V, after three different polarization times, for the 100 μF/40 V miniature aluminium electrolytic capacitor of Fig. 1. In the low voltage region of Fig. 2, the curves follow an approximate power law of the type $I \propto V^{3/2}$. The non-linearity between current and voltage in anodic oxides polarized at low voltages has been explained by a charge injection mechanism [5, 6]. It can be observed in Fig. 2 that for high fields, i.e. $V \gtrsim V_N$, the current depends exponentially on the voltage. The minimum, which shows at $V \gtrsim V_N$ in the I–V characteristics of Fig. 2 observed after 100 and 1000 s after applying the voltage, can be associated with the increase in the capacitor ESR mentioned before.

3.2. *a.c. characteristics*

The measurement of the dielectric characteristics in a range of frequencies gives further insight on the effects of applying to the capacitor voltages higher than V_N. Fig. 3 shows the variation of the equivalent series resistance (ESR) as a function of the reciprocal of the frequency for the 100 μF capacitor of Fig. 1 before (curve A) and after (curve B) recording the transients of Fig. 1. According to the model of McLean for an electrolytic capacitor [7], the ESR should depend linearly on the reciprocal of the angular frequency, ω, in the form:

$$\mathrm{ESR} = \frac{\tan \delta_{ox}}{\omega C} + R_c \qquad (2)$$

where C is the capacitance, $\tan \delta_{ox}$ represents the losses associated with the anodic oxide and R_c is the resistance attributed to the electrolyte, impregnating paper, contacts, etc. By using Equation 2 in the interpretation of the data of Fig. 3, it is concluded for instance that R_c undergoes a significant

Table 1. Time variation of the dielectric parameters of a 100 μF/40 V capacitor polarized at 60 V

	Time (min)			
	0	30	60	90
C_s (100 Hz) (μF)	117.0	119.3	119.4	118.9
$\tan \delta_{ox}$	0.0292	0.0385	0.0396	0.0416
R_c (ohm)	0.169	0.456	0.525	0.524

Table 2. Dielectric characteristics of different miniature aluminium capacitors subjected to a polarization of 1.5 times the nominal voltage for 30 min

Capacitor	C_s (μF)		$\tan \delta_{ox}$		R_c (ohm)	
	Before	*After*	*Before*	*After*	*Before*	*After*
47 μF/25 V	56.7	58.3	0.0322	0.0375	0.369	0.968
100 μF/25 V	119.4	120.8	0.0303	0.0335	0.133	0.173
33 μF/40 V	36.8	37.5	0.0313	0.0381	0.474	1.242
47 μF/40 V	60.3	61.6	0.0303	0.0440	0.289	0.727
100 μF/40 V	116.4	118.8	0.0339	0.0440	0.200	0.535

change from 0.113 to 0.280 ohm for curves A and B, respectively. However, the change on the capacitance is relatively small.

The effects of exposing the capacitors to high polarization voltages for definite times is better exemplified in Table 1 which shows the variation with time of C, $\tan \delta_{ox}$ and R_c of a typical 100 μF/40 V miniature aluminium capacitor polarized at 60 volts. As can be observed, there exists a continuous increase in $\tan \delta_{ox}$ and R_c while C remains almost constant. After only 90 min, $\tan \delta_{ox}$ and R_c have increased about 40 and 210%, respectively. A similar trend is obtained for other typical miniature capacitors, as shown in Table 2. In this case, the capacitors were polarized for 30 min at 1.5 times the nominal voltage.

4. Discussion

The transients of Fig. 1 for $V \lesssim V_N$ clearly show that the capacitor behaves as a nearly ideal capacitor, i.e. as a dielectric of low losses and a response function $\Phi = \Phi(t)$ given by Equation 1 with $n \simeq 1$. This is due in part to the fact that the permanent leakage current has a value well below the values of the currents detected in the measurements. As a consequence, the transport of charge through pinholes or microfissures in the dielectric layer should be very small. As for the detected transient currents in this low voltage region, it should be pointed out that a time dependence of the type of Equation 1 has been reported to occur in a large number of dielectrics. This kind of time dependence of the current has been usually attributed to the dielectric polarization currents [5] and/or the trapping of charge in the dielectric [6]. In our case, the first process seems much more likely since a transport of charge, either electronic or ionic, through the dielectric should produce an evolution of gases from the liquid electrolyte and this was not observed for $V < V_N$, even after long polarization times [8].

One of the main effects on the a.c. characteristics of exposing the miniature electrolytic capacitors to high voltages is, as shown in Figs. 1 to 3 and Tables 1 and 2, a large increase in the resistance associated to the electrolyte and a diminution in the resistance attributed to the dielectric (infinite in the ideal case). Simultaneously, there is a moderate increase in $\tan \delta_{ox}$ and C. These changes produced in the dielectric properties of the capacitors can be interpreted by a generalization of McLean's model of an electrolytic capacitor. The equivalent circuit which explains our results is shown in Fig. 4a where C is the capacitance of the corresponding ideal capacitor, R_{ox} is the resistance which takes into account the oxide dielectric losses, R_L is the resistance associated with the permanent leakage current through the oxide and R_c is the resistance of the contacts.

It is shown in the Appendix that the equivalent circuit proposed in this work for the miniature capacitors (Fig. 4a) can be made to correspond to McLean's series circuit (Fig. 4b) if:

$$C' = C\left(1 + \frac{1}{\omega^2 R_L^2 C^2}\right) \tag{3a}$$

$$\tan \delta'_{ox} \equiv \omega C' R'_{ox} = \tan \delta_{ox} + \frac{1}{\omega R_L C} \tag{3b}$$

(with $\tan \delta_{ox} \equiv \omega C R_{ox}$).

The increase of the tangent of the loss angle, $\tan \delta'_{ox}$, and the series capacitance, $C_S = C'$, observed in Tables 1 and 2 is in agreement with Equation 3 if one assumes that the value of the

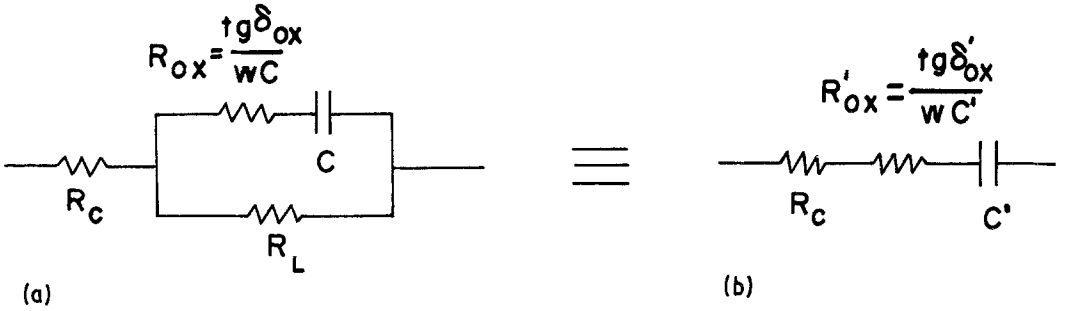

Fig. 4. (a) Proposed equivalent circuit for the miniature capacitors. (b) McLean series circuit for an electrolytic capacitor.

resistance R_L, which takes into account the transport of charge through the oxide, diminishes as a consequence of the damage produced by the high electric fields applied to the oxide. Simultaneously, it is supposed that the real capacitance, C, of the system remains practically constant. The change in the value of R_L, provoked by the polarization of the capacitors under stressed conditions, is attributed to the formation by the electric field of pores and microfissures as has been recently observed by scanning electron microscopy techniques [9]. It can be shown that the effect of the resistance R_L in Fig. 4a on the current transients consists in an increase of both the value of the response function $\Phi = \Phi(t)$ for $t = \infty$ and its time constant. These two characteristics become more and more apparent in Fig. 1 as the capacitors are exposed to increasing voltages.

A direct consequence of the damage produced in the oxide layer is that the permanent leakage current through the dielectric increases considerably. In this respect, it is known that the transport of charge across the oxide–electrolyte system produces the evolution of gases in the interior of the capacitor [8], a process which implies the consumption of protons from the electrolyte [10]. Therefore, at high polarization voltages, one should expect an increase of the contact resistance R_c. The curvature observed in the plot of Fig. 3 (curve B) at high frequencies is in agreement with the previous view, since an analysis of the capacitor system based in the transmission line model shows that this curvature can be related to an increase of the electrolyte resistivity in the interior of the tunnels in the aluminum foil [11, 12].

The exponential dependence of the current on the voltage for $V > V_N$ observed in Fig. 2 has been usually associated with an ionic conduction mechanism similar to the one present during the anodic oxidation in a forming electrolyte [3]. However, this interpretation has never been well documented, and is inconsistent with the increase in capacitance as a consequence of the application to the capacitor of voltages of up to $1.5V_N$. On the other hand, a series of recent works have shown that for electric fields close to the value of the field during anodization, there exists an appreciable electronic current, which might be the cause of dielectric breakdown in localized sites of the oxide [13, 14]. In this line, O'Dwyer [15] has shown that there might exist stable electronic conduction in an avalanche regime for values of the applied field below a critical value. In this case, the electronic conduction mechanism can be explained by an avalanche multiplication of electrons by impact ionization and this would lead to an exponential dependence of the current on the voltage. The above mechanisms of electronic conduction have also been employed to explain the processes of dielectric breakdown during the anodic oxidation (scintillation processes) where the primary electrons are injected through the electrolyte–oxide interface [13]. In the case of the capacitors under study, where the high voltages are applied to an anodic oxide immersed in an electrolyte of the impregnating type, the electronic conduction mechanism is greatly favoured by the high electrical conductivity and poor formation properties of these impregnating electrolytes in comparison to the ones used during the anodization process. The electronic current across the oxide, which increases exponentially with voltage, should give rise to scintillation processes for values of the electric field corresponding to values of the voltage higher than about V_N.

In conclusion, the experimental results observed

in this work for capacitors subjected to high polarization voltages, i.e. the change in the shape of the transients as well as the increase in the dielectric parameters (R_c, C and $\tan \delta_{ox}$), suggest that the conduction mechanism in the high voltage region is of the electronic type in an avalanche regime. This electronic current produces, in turn, an irreversible change in the electrical properties of the oxide and of the electrolyte.

Appendix

The impedance of the equivalent circuit of Fig. 4a, used in this work for representing the aluminium miniature electrolytic capacitors, is given by

$$Z = R_c + \frac{R_L}{1 + \omega^2(R_{ox} + R_L)^2C^2} + \frac{\omega^2 R_{ox}R_L(R_{ox} + R_L)C^2}{1 + \omega^2(R_{ox} + R_L)^2C^2} - j\frac{\omega R_L^2 C}{1 + \omega^2(R_{ox} + R_L)^2C^2}. \quad \text{(A1)}$$

When the capacitor dielectric parameters are measured with a bridge in the series mode, the real part of the impedance, $\mathrm{Re}[Z]$ represents the equivalent series resistance (ESR) and the imaginary part $\mathrm{Im}[Z]$ is given by $1/\omega C_s$ where C_s is the series capacitance. Therefore, the expressions of the capacitor ESR and C_s can be directly obtained from the expression of Z given by Equation A1. Assuming now that for a capacitor with low losses, $R_{ox}/R_L \ll 1$, one obtains for ESR and C_s

$$\mathrm{ESR} = R_c + \frac{R_L}{1 + \omega^2 R_L^2 C^2} + R_{ox}\frac{\omega^2 R_L^2 C^2}{1 + \omega^2 R_L^2 C^2} \quad \text{(A2)}$$

$$C_s = C + \frac{1}{\omega^2 R_L^2 C^2}. \quad \text{(A3)}$$

Introducing the parameters C' and $\tan \delta'_{ox}$ given by Equations 3 in the text, Equations A2 and A3 can be written in the form:

$$\mathrm{ESR} = R_c + \frac{\tan \delta'_{ox}}{\omega C'} = R_c + R'_{ox} \quad \text{(A4)}$$

$$C_s = C'. \quad \text{(A5)}$$

The Equations A4 and A5 allow one to assimiliate the series–parallel circuit of Fig. 4a to the McLean's series circuit of Fig. 4b.

Acknowledgements

We wish to thank BIANCHI, S. A. (Spain) and the Comisión Asesora de Investigación Científica y Técnica for the financial support of this work. One of us (CGA) acknowledges the Consejo Superior de Investigaciones Científicas for the grant awarded while working on this project. Also, we would like to thank Mr F. Serrano for his help in taking the measurements.

References

[1] V. Trifonova and A. Girginov, *J. Electroanal. Chem.* **107** (1980) 105.
[2] S. Ikonopisov, *Electrochim. Acta* **14** (1969) 761.
[3] A. Charlesby, *Proc. Phys. Soc. (London)* **66** (1953) 533.
[4] E. Loh, IEEE Trans. *Comp. Hyb. Manufac.* 4 (1981) 536.
[5] H. K. Jonscher, *J. Mater. Sci.* **16** (1981) 2037.
[6] C. J. Dell'Oca, D. L. Pulfrey and L. Young, in 'Physics of Thin Film' Vol. 6, Academic Press, New York (1971) p. 1.
[7] D. A. McLean, *J. Electrochem. Soc.* **108** (1968) 446.
[8] C. Gómez-Aleixandre, J. M. Albella and J. M. Martinez-Duart, submitted to *J. Electrochem. Soc.* (1982).
[9] K. Shimizu, G. E. Thompson and G. C. Wood, *Thin Solid Films* **92** (1982) 231.
[10] F. J. Burger and S. Viswanathan, *Electrochem. Technol.* **6** (1968) 189.
[11] R. H. Broadbent, *ibid.* **6** (1968) 163.
[12] A. R. Morley and D. S. Campbell, *Radio Electr. Eng.* **43** (1973) 421.
[13] S. Ikonopisov, *Electrochim. Acta* **22** (1977) 1077.
[14] J. M. Albella, I. Montero and J. M. Martinez-Duart, *Thin Solid Films* **58** (1978) 307.
[15] J. J. O'Dwyer, in 'Theory of Electrical Conduction and Breakdown in Solid Dielectrics', Clarendon Press, Oxford (1973).